

# Multi-hop Federated Private Data Augmentation with Sample Compression

Eunjeong Jeong<sup>1</sup>, Seungeun Oh<sup>1</sup>, Jihong Park<sup>2</sup>, Hyesung Kim<sup>1</sup>,  
Mehdi Bennis<sup>2</sup> and Seong-Lyun Kim<sup>1</sup>

<sup>1</sup>Electrical and Electronic Engineering, Yonsei University, Seoul, Korea

<sup>2</sup>Centre for Wireless Communications, University of Oulu, Finland

{ejjeong, seoh, hskim, slkim}@ramo.yonsei.ac.kr, {jihong.park, mehdi.bennis}@oulu.fi

## Abstract

On-device machine learning (ML) has brought about the accessibility to a tremendous amount of data from the users while keeping their local data private instead of storing it in a central entity. However, for privacy guarantee, it is inevitable at each device to compensate for the quality of data or learning performance, especially when it has a non-IID training dataset. In this paper, we propose a data augmentation framework using a generative model: *multi-hop federated augmentation with sample compression (MultiFAug)*. A multi-hop protocol speeds up the end-to-end over-the-air transmission of seed samples by enhancing the transport capacity. The relaying devices guarantee stronger privacy preservation as well since the origin of each seed sample is hidden in those participants. For further privatization on the individual sample level, the devices compress their data samples. The devices sparsify their data samples prior to transmissions to reduce the sample size, which impacts the communication payload. This preprocessing also strengthens the privacy of each sample, which corresponds to the input perturbation for preserving sample privacy. The numerical evaluations show that the proposed framework significantly improves privacy guarantee, transmission delay, and local training performance with adjustment to the number of hops and compression rate.

## 1 Introduction

Enhanced accessibility to big data has enabled machine learning (ML) and its further application as exemplified by on-device machine learning [Park *et al.*, 2018; McMahan *et al.*, 2017; Jeong *et al.*, 2018]. Individual devices are able to train a local model based on their private data, such as e-health medical records. Under limited communication resources and privacy constraints, it is a key challenge to achieve a ML model with high accuracy in real-life situations. Furthermore, each device is often scarce in samples and biased, i.e., non-IID across devices, which hampers generalization of the local model against unseen data samples.

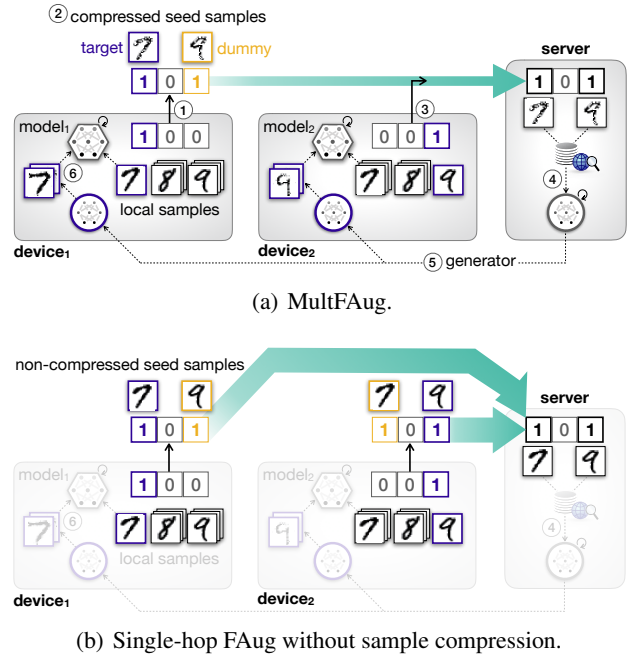


Figure 1: Comparison between (a) *multi-hop federated augmentation with sample compression (MultiFAug)* and (b) single-hop FAug without sample compression, for 2 devices associated with a server.

To cope with this, we proposed *federated augmentation (FAug)* in our preceding work [Jeong *et al.*, 2018], in which the devices collectively train and share a data sample generator. The associated edge server builds and trains a generator from a conditional generative adversarial network model (cGAN) [Mirza and Osindero, 2014], enabling each device to augment data samples by downloading the generator. The generator training at the server requires only a few seed samples collected from those devices. Thanks to these small number of seed samples, the scheme relieves communication overhead as well as privacy leakage compared to exchanging data samples directly across devices. However, it is inevitable to compensate privacy for uplink capacity. In other words, each device should upload more seed samples so as to reach strong privacy preservation by hiding their weaknesses in the large volume of samples.

In this paper, we propose a *multi-hop federated augmen-*

tation with sample compression (MultFAug) to improve both privacy guarantee and communication efficiency of on-device learning. Extending from the seed sample collection of FAug (see Figure 1(b)), multi-hop communication allows the devices to preserve privacy as they can hide their data distribution in the crowd. It also reduces the latency through succeeding short-distance transmissions (see Figure 1(a)). Namely, compressing seed samples reduces communication payload sizes while preserving more *sample privacy*, at the cost of compromising the quality of augmented samples. On the other hand, multi-hop communication allows each device to hide its data distribution over data labels, denoted as *label privacy*, in a communication-efficient way. These benefits are exemplified in Figure 1(a) describing the MultFAug operations as follows.

1. Out of 3 labels (digits 7, 8, 9),  $\text{device}_1$  lacks the samples of the *target label* 7. To preserve the label privacy by hiding its private sample distribution information (SDI)  $[1, 0, 0]$ ,  $\text{device}_1$  inserts a *dummy label* indicator into 9, yielding the public SDI  $[1, 0, 1]$ .
2.  $\text{device}_1$  compresses and appends two seed samples in 7 and 9 to its public SDI, and then transmit them to the next hop  $\text{device}_2$  (see Algorithm 1).
3.  $\text{device}_2$  has the target label 9. Its private SDI  $[0, 0, 1]$  can be hidden within the public SDI  $[1, 0, 1]$  of  $\text{device}_1$ . Therefore,  $\text{device}_2$  only forwards its received seed samples to the server.
4. After collection, the server first oversamples the seed samples (e.g., via Google’s image search for visual data) and then trains a generator model (see Algorithm 2).
5. Each device downloads the trained generator, and thereby locally augments the samples in the target labels for training its on-device ML model.

Compared to the original FAug, we numerically validate that the proposed MultFAug achieves the same test accuracy of the on-device ML model, with shorter communication latency while preserving more data privacy.

**Contribution.** Our contributions in this paper consist of two main idea as follow:

- *multi-hop communication.* We propose a data augmentation framework that improves communication efficiency and privacy preservation by adopting wireless transmission over multi-hop protocol.
- *data compression.* The deletion of randomly picked bits in data samples leads to less communication overhead and a stronger privacy guarantee for each data sample.

**Related works.** To address the lack of training data samples, it is common to locally oversample the original data, e.g., via rotating and masking for visual data [Park *et al.*, 2018], which may however struggle with locally biased samples. Exchanging data samples across different devices/servers is free from this problem, yet may incur huge communication overhead and/or violate data privacy [Balcan *et al.*, 2012]. Combination with federated learning alleviates the privacy violation problem [Yoshida *et al.*, 2019],

but makes a strong assumption that some devices are insensitive to privacy and willingly provide their data samples as proxy data. On the other hand, global proxy data can be either collected or gathered at the edge server [Zhang *et al.*, 2017; Huang *et al.*, 2018], yet it costs an additional effort to acquire such a dataset. Alternatively, generating synthetic data samples via generative adversarial networks (GANs) is a compelling data augmentation solution that guarantees data privacy while avoiding data exchanges [Sixt *et al.*, 2018; Zhu *et al.*, 2017]. These works however focus only on data sample privacy while neglecting SDI privacy and the impact on communication efficiency. In a similar manner, [Yonetani *et al.*, 2019] suggested a system wherein users with non-IID dataset train discriminators independently. However, these local discriminators reveal the data distribution of each user since they reflect the non-IIDness of the individuals. By contrast, our preceding work [Jeong *et al.*, 2018] only considers SDI privacy and communication efficiency, without incorporating data sample privacy guarantees. In this work, we fill such a gap by incorporating both SDI and data sample privacy, and investigate the effectiveness of multi-hop communications for preserving privacy in a more communication-efficient way.

## 2 Single-hop Federated Augmentation Without Sample Compression

In this section, we describe a baseline model FAug wherein every device is directly connected to the server. This will be extended in the next section to a multi-hop version of FAug, MultFAug.

With this in mind, we consider a server and a group of edge devices in a network. The devices are denoted by  $\mathcal{D} = \{1, 2, \dots, N\}$  with  $|\mathcal{D}| = N$ , and their locations are randomly selected following uniform random distribution.

The devices employs time division multiple access (TDMA), in which each device fully occupies the bandwidth allocated along its route. The total bandwidth is equally divided into the number of routes and therefore equal range of bandwidth is assigned to each route. The devices transmit signals over the air experiencing path loss and fading. Under the system bandwidth  $B$  and noise power spectral density  $N_0$ ,  $\text{device}_i$  sends samples with the instantaneous data rate  $B \log_2(1 + (g_i(t)P_i d_i^{-\alpha}/N_0B))$ , where  $g_i(t)$  is the fading coefficient,  $\alpha$  is the path loss exponent, and  $d_i$  denotes the distance between  $\text{device}_i$  and its direct destination. When a device transmits packets at a lower data rate than its channel capacity at the moment, it retransmits with infinite number of attempts. The transmission latency from  $\text{device}_i$  to the server, referred to as  $T_i$ , is calculated as the number of time slots required to transmit all of the seed samples.

Each device aims to train its learning model to classify data from its training set, which consists of image data samples and class labels corresponding to each sample. These class labels are discrete values tagged to a group of samples with common property. Let us assume that each device holds a non-IID training dataset; some of its class labels are deficient in data samples – referred to as *target labels*. In FAug, a device reports its missing labels to compensate for the target labels by uploading the seed samples to the server. When a

device picks up seed samples, it must include target samples that the device wants to replenish. As a first step, each device uploads its seed samples directly to the server. To avoid unnecessarily large communication payload in case of sending too many samples with the same labels, the device restricts the number of seed samples per label to a predetermined upper bound value  $b$ . The server oversamples these samples to train a conditional generative adversarial network (cGAN), one of the GAN variations in which extra information is additionally given as a condition for training both generator and discriminator [Mirza and Osindero, 2014]. When the training process ends, the devices receive the generator from the server. With the generative model, each device replenishes the target labels to achieve an IID training dataset.

During the transmission, the participants want to keep their local data private against the server. With this end, each device selects dummy samples, whose label is not the target one, from its own dataset and enclose them when sending target-labeled seed samples. This operation hides the target labels from the server as it cannot discriminate between the received target and dummy labels.

To address this label-wise privacy, we define the label privacy guarantee as the amount of label privacy preservation between interconnected nodes. Let  $\mathbf{y}_i^T$  be a 1-dimensional logical vector whose elements are the target labels (private SDI) of  $\text{device}_i$  that the server successfully receives. Similarly,  $\mathbf{y}_i$  is a vector of labels including dummy labels (public SDI). Then, the label privacy of  $\text{device}_i$  guaranteed from the server  $\text{Priv}_i^{(1)}$  is defined as

$$\text{Priv}_i^{(1)} = 1 - \frac{|\mathbf{y}_i^T|}{|\mathbf{y}_i|} \quad (1)$$

where  $|\cdot|$  indicates the sum of all elements of a vector. A device can keep its dataset information (represented as class label distribution) more private if it includes more dummy labels, while the label privacy guarantee is constrained by a ratio of target to non-target labels. Note that if a device fails to upload part of its seed samples, the server does not receive the label corresponding to the failed sample. This incomplete leads to a weaker guarantee for the device's label privacy due to the reduced number of dummy labels.

The overall latency in single-hop FAug is calculated as the transmission delay until the seed samples from all participants arrive at the server. In other words, the longest delay among all devices equals to the overall latency of the system. The overall uplink latency is measured as

$$L^{(1)} = \max_{i \in \mathcal{D}} \{T_i\} \quad (2)$$

Since the last arriving seed sample decides the overall latency, devices located far away are prone to path loss, which undermines the training step at the server.

### 3 Multi-hop Federated Augmentation With Sample Compression

The single hop FAug has inherent problems in terms of privacy leakage for target labels and small uplink coverage. To tackle these issues, we propose a *multi-hop federated augmentation with sample compression (MultFAug)* where devices construct a multi-hop route to the destination server and

Variable	Description
$N$	Number of devices ( $ \mathcal{D}  = N$ )
$M$	Max. number of hops in the system
$R_j$	Set of devices transmitting through $j^{\text{th}}$ route ( $R_j \subset \mathcal{D}$ )
$r$	Number of total routes ( $\max r = \lfloor \frac{N}{M} \rfloor$ )
$f^m(i)$	$m$ -hop destination of $\text{device}_i$ ( $f^0(i) = i$ )
$\rho$	Compression rate
$Q_\rho$	Compression mechanism with rate $\rho$
$T_i$	Latency
$\tau$	Deadline threshold ( $T_i \leq \tau$ for $\forall i$ )
$\mathbf{y}_i^T$	Target label indicator (private SDI) of $\text{device}_i$
$\mathbf{y}_i^{\text{dum}}$	Dummy label indicator of $\text{device}_i$
$\mathbf{y}_i$	Total label indicator (public SDI) of $\text{device}_i$ ( $= \mathbf{y}_i^T \vee \mathbf{y}_i^{\text{dum}}$ )
$\mathcal{X}_i$	Set of data samples that $\text{device}_i$ wants to send
$\hat{\mathcal{X}}_i$	Set of compressed data samples in $\text{device}_i$
$l$	Label privacy threshold ( $ \mathbf{y}_i^{\text{dum}}  < l$ )
$b$	Number of seed samples per label (upper bound)

Table 1: Notation and description in MultFAug

transmit their own compressed target samples. The proposed MultFAug hides sources of target samples from an aggregating server and intermediate devices, while guaranteeing the privacy leakage of individual delivered samples. Furthermore, this multi-hop feature extends the range of FAug by associating more devices to the server via multi-hop device-to-device communications, as elaborated in the following subsections.

#### 3.1 Multi-hop Protocol

We leverage multi-hop communications in order to increase coverage of the devices and provides higher privacy guarantee. Multi-hop communications can reduce uplink latency by exploiting multiple successes of short path between devices. Especially, a device at the edge of the coverage stops suffering from sequential transmission outage if the multi-hop communications is applied. In addition, this multi-hop feature makes the server unable to discriminate the original source device of received each target labels because it receives only a mixed set of target labels and samples. This is consistent for intermediate devices. The proposed protocol of the multi-hop FAug is elaborated as follows.

Let us assume that the route from devices to the server is configured by the system. For a given routing path, a device sends its seed samples to another device as a relay node towards the server. Devices on the same route accumulate their samples over hops as described in Algorithm 1. As a result, devices located nearby the server have to carry more samples than those distant from the server. When a relaying node receives samples with public SDI, it attaches its own seed samples and overwrites their labels onto the public SDI. In this research, the devices are interconnected with fixed number of hops. As in the single hop FAug, each device avoids sending more than  $b$  samples that share the same labels. If the target label of  $\text{device}_i$  is already in the public SDI ( $\mathbf{y}_i$ ), it discards random samples in its target label and replaces them from its local training set, so that any samples of the labels in  $\mathbf{y}_i$  do

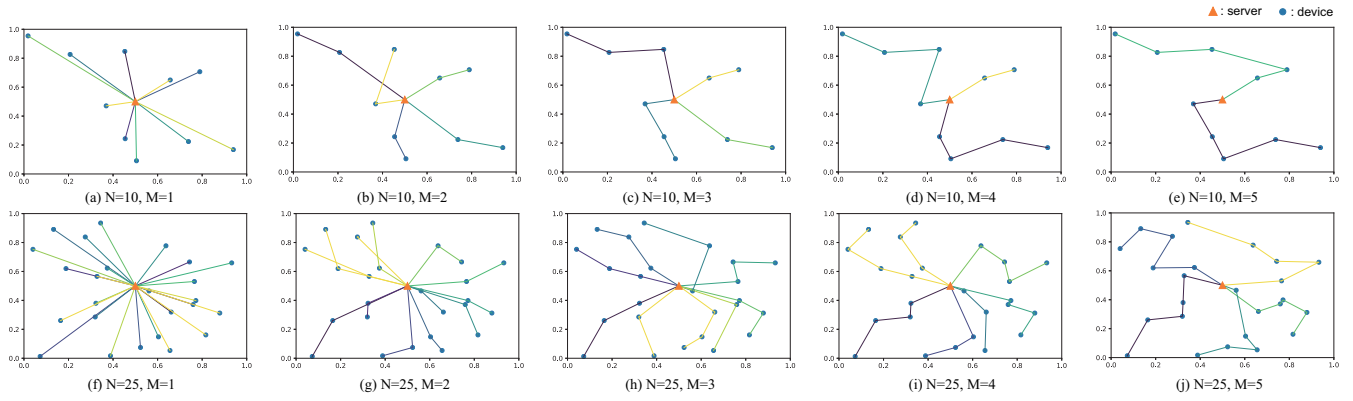


Figure 2: Exemplary topologies of single-hop and multi-hop scenarios with respect to the number of devices and maximum hops ( $N = \{10, 25\}$ ,  $M = 1, 2, \dots, 5$ )

not exceed  $b$ . If an intermediate device receives an aggregated seed samples that already include its target label, the device does not add any dummy label at its transmission phase.

Consider a function  $f : \mathcal{D} \rightarrow \mathcal{D}$  that outputs an index of a device's direct destination through its route. Following this definition, the index of  $\text{device}_i$ 's direct destination is  $f(i)$ . Likewise, its  $m$ -hop destination is  $f^m(i)$ . The target labels of  $\text{device}_i$  is label-private against its  $M$ -hop destination, and the label privacy guarantee is

$$\text{Priv}_i^{(M)} = 1 - \frac{|\mathbf{y}_i^T|}{\left| \bigvee_{m=0}^M \mathbf{y}_{f^m(i)} \right|} \quad (3)$$

When the relaying transmissions succeed in a row, the seed sample set becomes larger as the seed samples are accumulated across the devices. Accordingly, total labels that the  $M$ -hop destination receives grows, i.e.,  $|\mathbf{y}_i| \leq |\mathbf{y}_i \vee \mathbf{y}_{f(i)}| \leq \dots \leq |\bigvee_{m=0}^M \mathbf{y}_{f^m(i)}|$ . This trend does not appear clearly when a device partially or fully fails to send its seed samples under tight communication constraints.

The latency in MultFAug is denoted as  $T_i$ , which occurs between  $\text{device}_i$  and its relaying device. None of the two devices in the same route occupy the bandwidth at the same time. The server waits for sample arrival from all routes. Assume that there are  $r$  different routes and each of them binds at most  $M$  devices delivering the seed samples through  $M$ -hop relays. The latency in a route is calculated as the sum of latency at each hop. The overall latency in the system using a multi-hop protocol is

$$L^{(M)} = \max_{j \in \{1, 2, \dots, r\}} \sum_{i \in R_j} T_i \quad (4)$$

where  $R_j$  indicates the  $j^{\text{th}}$  route. The overall latency in (2) is thereby interpreted as a special case in which  $M = 1$ . In single hop protocol, the number of routes is the same as that of devices because each device independently has its own route to the server. That is, all  $T_{R_j} = \sum_{i \in R_j} T_i$  is identical to  $T_i$ .

### 3.2 Sample Compression

We include a compression mechanism in the proposed protocol in order to reduce the communication overhead and pri-

**Algorithm 1**  $\text{Device}_i$ 's sample compression and transmission for target and dummy labels in MultFAug

**Require:**  $R_j = \{i | i = 1, 2, \dots, M\}$  ( $j = 1, \dots, r$ ) where  $i = 1$  is the edge device of  $j^{\text{th}}$  route and  $f(i) = i + 1 \forall i$ , label privacy threshold  $l$ , compression rate  $\rho$

```

1: for  $j = 1$  to  $r$  do
2:   while  $i < M$  do
3:     if  $d$  then
4:        $\mathcal{X}_i \leftarrow \mathcal{X}_i^T \cup \mathcal{X}_i^{\text{dum}}$ 
5:        $\hat{\mathcal{X}}_i \leftarrow Q_\rho(\mathcal{X}_i)$ 
        (Compress  $\mathcal{X}_i$ )
6:        $\mathbf{y}_i \leftarrow \mathbf{y}_i^T \vee \mathbf{y}_i^{\text{dum}}$ 
7:     else
8:       Receive  $\mathcal{X}_{i-1}, \mathbf{y}_{i-1}$ 
9:       if  $|\mathbf{y}_{i-1} \vee \mathbf{y}_i^T| \leq l$  then
10:         $\mathcal{X}_i, \mathbf{y}_i \leftarrow \mathcal{X}_{i-1}, \mathbf{y}_{i-1}$ 
11:      else
12:        Set  $\mathbf{y}_i^{\text{dum}}$  such that  $|\mathbf{y}_i^{\text{dum}}| \leftarrow l - |\mathbf{y}_{i-1} \vee \mathbf{y}_i^T|$ 
13:         $\mathcal{X}_i \leftarrow \mathcal{X}_i^T \cup \mathcal{X}_i^{\text{dum}}$ 
14:         $\hat{\mathcal{X}}_i \leftarrow Q_\rho(\mathcal{X}_i)$ 
15:         $\mathbf{y}_i \leftarrow \mathbf{y}_i^T \vee \mathbf{y}_i^{\text{dum}}$ 
16:      end if
17:    end if
18:    Transmit  $\mathcal{X}_i$  to  $\text{device}_{i+1}$ 
19:  end while
20:  Transmit  $\mathcal{X}_M$  to the server
21: end for

```

vacuity leakage of each seed sample. Specifically, each device compresses its own sample to be delivered by discarding randomly selected bits from the sample. The number of the selected bits is determined by a compression rate  $\rho$ , which is decided a priori. Note that the similarity between two compressed samples becomes larger compared to that between the original ones. This indicates that the sample compression makes it more difficult to distinguish those samples, leading to stronger local privacy preservation.

For both sample privacy and communication efficiency, each device discards some of the bits from the data sam-

---

**Algorithm 2** Server’s sample collection, oversampling, and cGAN training.

---

**Require:** deadline threshold  $\tau$ , route  $R_j(j = 1, 2, \dots, r)$

- 1: **for**  $t = 1$  to  $\tau$  **do**
- 2:   **for all**  $R_j$  **do**
- 3:     **if**  $\mathcal{X}_j$  arrived through  $R_j$  **then**
- 4:       samples  $\leftarrow$  samples  $\cup \mathcal{X}_j$
- 5:        $\mathbf{y} \leftarrow \mathbf{y} \vee \mathbf{y}_j$
- 6:     **end if**
- 7:   **end for**
- 8: **end for**
- 9: real samples  $\mathcal{X}_{real} \leftarrow$  Oversample data with  $\mathbf{y}$
- 10: **while**  $G$ ’s parameters have not converged **do**
- 11:   Select a random batch from the real samples
- 12:   Generate noise  $\mathbf{z} \sim p(\mathbf{z})$
- 13:   Generate synthetic samples  $\mathcal{X}_{gen} \leftarrow G(\mathbf{z}, \mathbf{c})$
- 14:   Calculate loss with real samples  
 $D_{loss} = \log D(\mathcal{X}_{real}|\mathbf{c})$
- 15:    $\mathbf{c}_{SDI} \leftarrow \mathbf{y}$
- 16:   Calculate loss with synthetic samples  
 $G_{loss} \leftarrow \log(1 - D(G(\mathbf{z}|\mathbf{c}_{SDI})))$
- 17: **end while**
- 18: **return**  $G$
- 19: **for all**  $i$  **do**
- 20:   Transmit  $G$  to  $i$
- 21: **end for**

---

ples. The number of removing bits depends on the compression rate  $\rho$ . The sample distortion also results in obfuscation between two different images as the image similarity increases. The difficulty in distinguishing those samples leads to stronger local privacy preservation.

Specifically, the proposed sample compression consists of sparsification and transformation to a compressed sparse row matrix. At first, we provide a randomized sparsification algorithm denoted by  $Q_\rho : X \rightarrow \hat{X}$  where  $X$  and  $\hat{X}$  indicates the set of bits composing the original sample and its sparsified version, respectively. Let us consider that the devices train with the MNIST dataset in the MultFAug system. Among  $28 \times 28$  elements of a handwritten image,  $\lfloor \rho \times 28 \times 28 \rfloor$  arbitrary elements are chosen and converted to zero. After converting partial elements into zero with rate  $\rho$ , the device compresses each of the distorted sample into a sparse matrix, resulting in smaller data size. Specifically, the devices transmit their seed samples as a form of compressed sparse row (CSR) matrices that consist of the original matrices’ nonzero elements, list of row and column indices for the nonzero elements [Saad, 2003]. Hence if a distorted sample contains a number of zero values, its sparse matrix saves on communication payload. The data size of  $\hat{x}$  averages out at 1/5 of the original data size, although it varies according to the number of nonzero elements in each data sample. The reduction of data size lessens communication payload and therefore achieves less latency.

When devices transmit their data samples to the relaying device, they disclose their local information. In case of transmitting through multiple hops, the local information inevitably reaches the server. Therefore, a device locally dis-

torts its data samples before uploading it to restrict the leakage of local information.

Local differential privacy (local DP) is provided in contexts where each participant distorts its local data samples to keep them private before they reach to other entities [Kairouz *et al.*, 2014]. While samples guaranteed local DP need distortion at every element of each sample, our sample compression removes partial elements of a sample to increase the similarity of the samples in the dataset. Therefore, we suggest a measure of sample privacy guarantee inspired from local DP. Local differential privacy implies that the output reveals the limited information of the input. If any data sample  $x, \tilde{x}$  in the original dataset  $\mathcal{X}$  transform into identical output  $\hat{x}$  among the codomain  $\hat{\mathcal{X}}$  with higher probability, it infers that the mechanism privatizes each sample from the others more strictly [Xiong *et al.*, 2016]. For a non-negative  $\epsilon$ , a privatization mechanism  $Q$  is  $\epsilon$ -locally differentially private if  $\max_{(x, \tilde{x}, \hat{x}) \subset \mathcal{X} \times \mathcal{X} \times \hat{\mathcal{X}}} \{Q(\hat{x}|x)/Q(\hat{x}|\tilde{x})\} \leq e^\epsilon$ . In similar fashion, our randomized compression mechanism  $Q$  yields high image similarity between any two different data samples: for any  $x, \tilde{x}$  in the dataset, the distance between their output  $Q_\rho(x)$  and  $Q_\rho(\tilde{x})$  is short.

The sample privacy guarantee of the dataset is defined as the inverse of image similarity. Without loss of generality, the image similarity of data samples in the accumulated dataset  $\mathcal{X}$  is measured as

$$\text{sim}(\mathcal{X}) = \max_{(x, \tilde{x}) \subset \mathcal{X} \times \mathcal{X}} \log d(Q_\rho(x), Q_\rho(\tilde{x})) \quad (5)$$

for any  $x, \tilde{x}$ . To measure the similarity in (5), we apply classical multidimensional scaling (MDS) algorithm, a statistical technique used to represent each image by a point in a lower dimensional space. To find the configuration in the low-dimensional space, the loss function in MDS called *stress* should be minimized. It is known that the direct solution for the classic MDS problem exists when the pairwise distances of converted samples are calculated as Euclidean distance. The configured map displays the optimal distances among the converted points, which visualizes the level of similarity [Mair, 2018; Hout *et al.*, 2016].

## 4 Numerical Results

In this section, we numerically evaluate the performance of the proposed MultFAug, in terms of its communication efficiency and privacy guarantee. The network topologies under study is visualized in Figure 2.

### 4.1 Experimental Settings

Namely, we consider  $N = \{10, 25\}$  devices that are uniformly distributed over a two-dimensional network plane with the size  $10 \times 10\text{km}^2$ . From a single server located at the center of the plane, multiple device-to-server routes are constructed in a nearest-neighbor rule, in a way that each route comprises up to  $M \leq 5$  hops. Every device therein has 1,804 MNIST samples with 10 labels, comprising 4 samples in a single target label and 200 samples for each non-target label. Each device’s target label is uniformly randomly selected, leading to the non-IID MNIST dataset dispersed across devices. The edge devices can bound the minimum

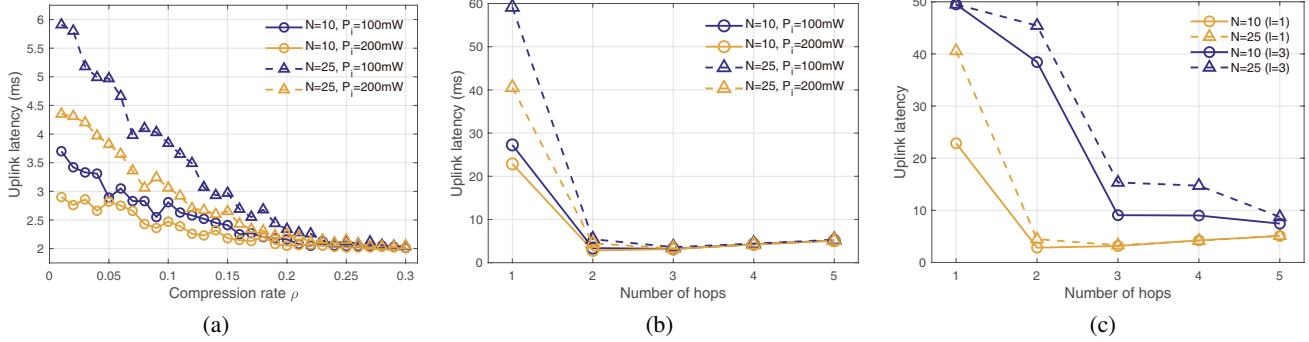


Figure 3: Uplink latency with respect to (a) compression rate  $\rho$  with different transmission powers, (b) the number of hops with different transmission powers, (c) the number of hops with different label privacy thresholds  $l$  ( $\rho = 0.02$ ).

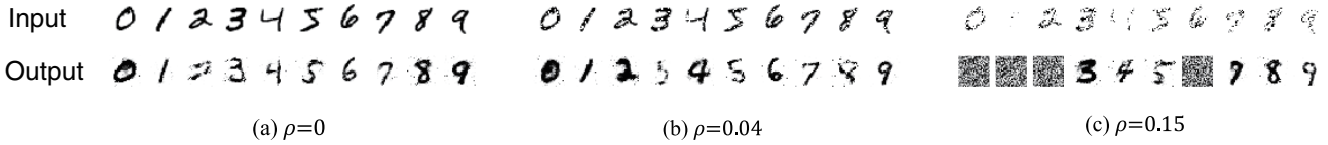


Figure 4: Input and output samples of the generator, which is a part of the trained cGAN in the server for different compression ratios: (a)  $\rho = 0$ , (b)  $\rho = 0.04$ , and (c)  $\rho = 0.15$ .

amount of their label privacy guarantee by adding  $l$  dummy label(s). For instance, setting  $l = 1$  by default brings about  $1 - (|\mathbf{y}_i^T|/|\mathbf{y}_i|) = 1/2$  for any  $i \in \mathcal{D}$ . This implies that the label privacy of each device is bounded to 0.5 in direct transmission between any two devices. The communication and privacy performance is evaluated based on a reference device, the farthest device from the server within a route that is uniformly randomly selected. The reference device represents the tendency of all devices by averaging the results with sufficient amount of iterations.

For MultFAug, the server trains a cGAN [Mirza and Osindero, 2014] consisting of a 4-layer discriminator network, as well as a 4-layer generator network with 1,493,520 weight parameters. During local training after MultFAug, following [Jeong *et al.*, 2018], each device utilizes a convolutional neural network with 1,199,776 weight parameters, consisting of 2 convolutional layers, 1 max-pooling layer, 1 flattened layer, and 2 fully connected layers. Other default simulation settings are summarized as follows:  $\alpha = 4$ ,  $B = 20\text{MHz}$ ,  $P_i = 200\text{mW}$ ,  $N_0 = -174\text{dBm/Hz}$ ,  $h^2 \sim \exp(1)$ .

## 4.2 Uplink Latency

Figure 3(a) illustrates that more sample compression ratio  $\rho$  tends to decrease the reference device's uplink latency, thanks to the communication payload size reduction. The latency has a minor fluctuation over  $\rho$ , since lower  $\rho$  does not always yield smaller CSR format data sizes (see the details in Sec. III-B). The latency under  $N = 25$  is higher than that of  $N = 10$  due to its more accumulated volume of seed samples, as also observed in Figure 3(b). Figure 3(b) shows that the uplink latency from the reference device to the server is minimized at 2 hops for  $N = 10$  or 3 hops for  $N = 25$ .

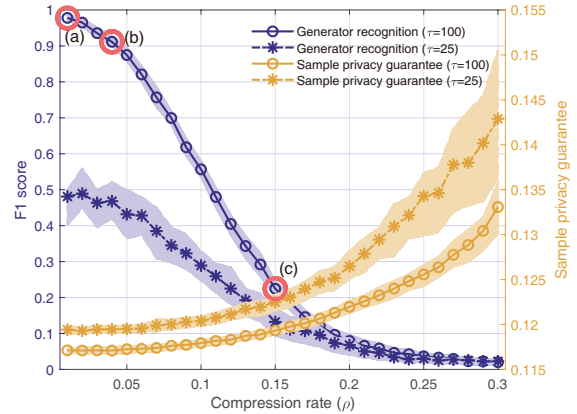
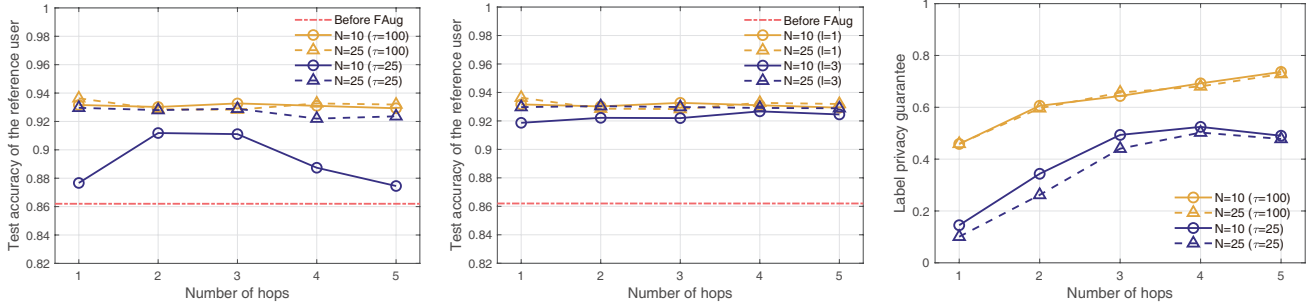


Figure 5: Trained generator's F1 score (left, violet) and sample privacy guarantee (right, yellow) with respect to sample compression rate  $\rho$  ( $N = 10$ ,  $M = 2$ ).

The latency is convex-shaped with respect to the number  $M$  of hops due to the following two conflicting behaviors. On the one hand, as  $M$  increases, path losses are compensated thanks to the per-hop distance reduction. On the other hand, more hops are likely to incur more channel outages, while increasing the accumulated volume of seed samples from the preceding hops. Figure 3(c) demonstrates the influence of minimum number of dummy labels on the overall latency. The latency is higher in a system that provides stronger label privacy in every direct transmission because of the increased number of seed samples to transmit.





(a) Test accuracy with latency deadlines ( $\tau$ ). (b) Test accuracy with label privacy guarantee ( $l$ ). (c) Label privacy guarantee with latency deadlines.

Figure 6: Evaluations with respect to the number of hops  $M$ . Test accuracy of the reference user after operating FAug in single hop and multi-hop protocols with different (a) latency thresholds, (b) label privacy guarantee thresholds, (c) label privacy guarantee with different latency thresholds ( $\rho = 0.02$ ).

### 4.3 Generator Performance

For different  $\rho$ 's, Figure 4 visualizes the aggregated seed samples at the server, i.e., the input samples for cGAN training. Each output sample of the trained cGAN's generator is obtained by feeding a Gaussian noise and a class label. With  $\rho = \{0, 0.04\}$ , the generator can successfully produce augmented digits. On the contrary, with  $\rho = 0.15$ , the generator fails to yield augmented samples for the digits 0, 1, 2, and 6, highlighting the importance of optimizing  $\rho$ .

Figure 5 shows the performance of the trained generator (left, violet) and sample privacy guarantee (right, yellow) with respect to  $\rho$ . The generator's performance is measured using the F1 score that is the harmonic mean of precision and recall, where precision increases with the similarity between the generated and ground-truth images, and recall increases with the number of generable images. As  $\rho$  increases, while the sample privacy guarantee increases, the cGAN is trained with more noisy samples, degrading the trained generator's F1 score. With a more stringent sample collection latency deadline  $\tau$ , the server collects fewer seed samples, leading to the generator's lower F1 score while increasing the sample privacy guarantee.

### 4.4 Test Accuracy of Local Models After MultFAug

Lastly, Figure 6(a) and 6(b) illustrate the reference device's test accuracy before and after applying MultFAug with respect to the number of hops. With a long collection latency deadline  $\tau$  and/or a large number of devices, the server can collect a sufficiently large number of seed samples for training the generator of MultFAug. The plenty of seed samples also improve the reference device's local training after applying MultFAug. Therefore, the abundance of acquired seed samples enables the device to achieve high test accuracy, regardless of the communication protocol characterized by the number of hops. On the contrary, with a more stringent latency deadline  $\tau = 25$ , the test accuracy is maximized at around 2-3 hops that provide the minimum uplink latency as observed in Figure 3(b). When the deadline is tighter, the

number of hops weighs heavier with the range of the amount of arrived seed samples. Therefore, the inverse tendency is shown in uplink latency and test accuracy.

In contrast, label privacy guarantee increases with the number of hops, as shown by Figure 6(c). Note that the larger number of hops does not always ensure the stronger label privacy, specifically in the cases under tighter time deadlines. For instance, when the latency deadline is  $\tau = 25$ , the server is less likely to receive all seed samples in time. The multi-hop protocol makes each sample to pass through more devices, although it has an advantage of shortening the travel distance of each sample per one transmission. As a result, devices with a tighter latency deadline show concave curves with an optimal  $M = 4$ .

## 5 Conclusion

In this paper, we proposed a multi-hop federated augmentation with sample compression (MultFAug) scheme. MultFAug allows devices to augment data samples by hiding their target labels in multi-hop communications while reducing the device-to-server uplink latency. In addition, the sample compression of MultFAug preserves the privacy of each seed sample, and reduces the communication overhead at the same time. The effectiveness of MultFAug was validated by numerical evaluations, highlighting the importance of the number of hops and compression rate. For a given network topology and channel condition, jointly optimizing the number of hops and compression rate could thus be an interesting topic for future work.

## Acknowledgements

This research was supported partly by Basic Science Research Program through the National Research Foundation of Korea(NRF) funded by the Ministry of Science and ICT(NRF-2017R1A2A2A05069810), partly by Academy of Finland projects SMARTER, CARMA, and 6Genesis Flagship (grant no. 318927), and partly by AIMS and ELLIS projects at the University of Oulu.

## References

- [Balcan *et al.*, 2012] Maria F. Balcan, Avrim Blum, Shai Fine, and Yishay Mansour. Distributed learning, communication complexity and privacy. In *Conference on Learning Theory*, pages 26–1, 2012.
- [Hout *et al.*, 2016] Michael C. Hout, Hayward J. Godwin, Gemma Fitzsimmons, Arryn Robbins, Tamaryn Menneer, and Stephen D. Goldinger. Using multidimensional scaling to quantify similarity in visual search and beyond. *Attention, Perception, & Psychophysics*, 78(1):3–20, 2016.
- [Huang *et al.*, 2018] Li Huang, Yifeng Yin, Zeng Fu, Shifa Zhang, Hao Deng, and Dianbo Liu. Loadaboost: Loss-based adaboost federated machine learning on medical data. *arXiv preprint arXiv:1811.12629*, 2018.
- [Jeong *et al.*, 2018] Eunjeong Jeong, Seungeun Oh, Hye-sung Kim, Jihong Park, Mehdi Bennis, and Seong-Lyun Kim. Communication-efficient on-device machine learning: Federated distillation and augmentation under non-iid private data. *arXiv preprint arXiv:1811.11479*, 2018.
- [Kairouz *et al.*, 2014] Peter Kairouz, Sewoong Oh, and Pramod Viswanath. Extremal mechanisms for local differential privacy. In *Advances in Neural Information Processing Systems (NeurIPS)*, pages 2879–2887, 2014.
- [Mair, 2018] Patrick Mair. Multidimensional scaling. In *Modern Psychometrics with R*, pages 257–287. Springer, 2018.
- [McMahan *et al.*, 2017] H. B. McMahan, E. Moore, D. Ramage, S. Hampson, and B. A. y Arcas. Communication-efficient learning of deep networks from decentralized data. In *Proc. of AISTATS*, Fort Lauderdale, FL, USA, April 2017.
- [Mirza and Osindero, 2014] Mehdi Mirza and Simon Osindero. Conditional generative adversarial nets. *arXiv preprint arXiv:1411.1784*, 2014.
- [Park *et al.*, 2018] Jihong Park, Sumudu Samarakoon, Mehdi Bennis, and Mérouane Debbah. Wireless network intelligence at the edge. *submitted to Proc. IEEE. ArXiv preprint: <https://arxiv.org/abs/1812.02858>*, 2018.
- [Saad, 2003] Yousef Saad. *Iterative methods for sparse linear systems*, volume 82. Siam, second edition, 2003.
- [Sixt *et al.*, 2018] Leon Sixt, Benjamin Wild, and Tim Landgraf. Rendergan: Generating realistic labeled data. *Frontiers in Robotics and AI*, 5:66, 2018.
- [Xiong *et al.*, 2016] S. Xiong, A. D. Sarwate, and N. B. Mandayam. Randomized requantization with local differential privacy. In *2016 IEEE International Conference on Acoustics, Speech and Signal Processing (ICASSP)*, pages 2189–2193, March 2016.
- [Yonetani *et al.*, 2019] Ryo Yonetani, Tomohiro Takahashi, Atsushi Hashimoto, and Yoshitaka Ushiku. Decentralized learning of generative adversarial networks from multi-client non-iid data. *arXiv preprint arXiv:1905.09684*, 2019.
- [Yoshida *et al.*, 2019] Naoya Yoshida, Takayuki Nishio, Masahiro Morikura, Koji Yamamoto, and Ryo Yonetani. Hybrid-fl: Cooperative learning mechanism using non-iid data in wireless networks. *arXiv preprint arXiv:1905.07210*, 2019.
- [Zhang *et al.*, 2017] Chaoyun Zhang, Xi Ouyang, and Paul Patras. Zipnet-gan: Inferring fine-grained mobile traffic patterns via a generative adversarial neural network. In *Proceedings of the 13th International Conference on emerging Networking EXperiments and Technologies*, pages 363–375. ACM, 2017.
- [Zhu *et al.*, 2017] Xinyue Zhu, Yifan Liu, Zengchang Qin, and Jiahong Li. Data augmentation in emotion classification using generative adversarial networks. *arXiv preprint arXiv:1711.00648*, 2017.